ERASMUS MUNDUS JOINT MASTERS DEGREE

SERP+ PROGRAMME (Surface, Electro, Radiation and Photochemistry+)

Photophysical Investigations on Molecular systems leading to Singlet Fission processes.

Authored by SANDRA MERIN SEBASTIAN

Supervisors: Dr. Minh-Huong Ha-Thi and Dr. Thomas Pino

A thesis submitted in partial fulfillment of the requirements for a degree of

MASTER OF SCIENCE

Université Paris-Saclay

Institut des Sciences Moléculaires d'Orsay – ISMO

July 2024

Table of Contents

Abstract

Solar energy is one of the cleanest and most renewable sources of energy available, increasing the efficiency of which is beneficial economically and environmentally. Multiple exciton generation is one of the ways to achieve this, of which singlet fission comes out to have the highest theoretical efficiency up to 200%. Singlet fission (SF) is an ultrafast, spin-allowed process by which a high-energy singlet exciton splits into two triplet excitons. The process of singlet fission can improve the efficiency of solar cells by exceeding the existing Shockley-Queisser limit to 45%. Several molecules in acenes and rylene families are excellent systems for singlet fission studies, which yield a theoretical triplet quantum yield of 200%. In this thesis, we did extensive preliminary studies on such molecules, particularly, TIPS Pentacene, TIPS Tetracene, and TIPS Anthracene. Hydrodynamic size measurements of nanoparticles were measured using the Dynamic Light Scattering technique and their morphological analysis was carried out using Scanning electron microscopy. Nanosecond transient absorption spectroscopy was employed to study the formation and the lifetimes of the triplet state both in solutions and nanoparticles. The triplet quantum yield of the same was determined by relative actinometry using $[Ru(bpy)_3]^{2+}$.

Résumé

L'énergie solaire est l'une des sources d'énergie les plus propres et les plus renouvelables disponibles, dont l'augmentation de l'efficacité est bénéfique sur le plan économique et environnemental. La génération d'excitons multiples est l'un des moyens d'y parvenir, dont la fission singulet se révèle avoir l'efficacité théorique la plus élevée jusqu'à 200 %. La fission singulet (SF) est un processus ultrarapide autorisé par spin par lequel un exciton singulet à haute énergie se divise en deux excitons triplet. Le processus de fission singulet peut améliorer l'efficacité des cellules solaires en dépassant la limite Shockley-Queisser existante à 45 %. Plusieurs molécules des familles des acènes et des rylènes constituent d'excellents systèmes pour les études de fission singulet, qui donnent un rendement quantique théorique de triplet de 200 %. Dans ce travail, nous avons réalisé des études préliminaires approfondies sur des molécules de la famille d'acènes, en particulier le TIPS Pentacène, TIPS Tétracène et TIPS Anthracène. Les mesures de taille hydrodynamique des nanoparticules ont été mesurées à l'aide de la technique de diffusion dynamique de la lumière (DLS) et l'analyse morphologique a été réalisée par microscopie électronique à balayage. La spectroscopie d'absorption transitoire nanoseconde a été utilisée pour étudier la formation de l'état triplet, ainsi que leur durée de vie dans des solutions et des nanoparticules. Le rendement quantique de formation des triplets a été déterminé par actinométrie relative en utilisant $[Ru(bpy)_3]^{2+}$.

Acknowledgments

First and foremost, I would like to thank my supervisor Dr. Minh-Huong Ha-Thi for making me confident in the experiments and for her valuable guidance and teachings. She has been always available whenever I had a difficulty whether during the experiments or the data interpretation. I am also grateful for the journal club, weekly presentations, and discussions with Dr. Thomas Pino and Dr. Karine Steenkeste, their valuable thoughts and insights were always been helpful and motivating to go on and for helping me with several spectroscopic instrumentation techniques. I would like to thank you for giving me the chance to do femtosecond experiments at the University of Lorraine, Nancy, and thereby to have an idea of the femto experiments.

I'd also like to thank Farah Savina for her valuable help throughout, along with her busy schedule, from teaching me the synthesis, distillation, and DLS, and helping me get the SEM measurements with Frank Fortuna. I would like to express my gratitude towards Prof. Rachel Meallet-Renault for her insightful critical comments and discussions during the meetings, which helped me to think deeper, and for helping me with the hard sphere experiments. Mariah was also a constant support for me throughout the experiments with the hard-sphere while preparing her poster.

Thank you to all my friends at ISMO, especially Daniel and My for your support and motivation during my experiments and for helping me with solving the problems I encountered during the transient absorption experiments and making me able to do it with full confidence.

I would like to take this opportunity to thank Dr. Vibha Sharma for being my co-referee from India for this thesis. I am grateful to all my friends and teachers from the school, Bachelors and Masters, for giving me the best stepping stones to reach at this moment.

In addition, I am profoundly grateful to the Erasmus Mundus Programme, through which I got the chance to attend my semesters at prestigious universities around Europe, especially, Universite Paris Saclay, Universidade do Porto and Adam Mickiewicz University, Poznan and getting an opportunity to do my master thesis at ISMO, Orsay.

I would like to extend my sincere gratitude to Prof. Sandrine Lacombe, Prof. Edwardo.F. Marques and Prof. Tomez Pedzinski for their words of wisdom of all time.

Last, but not least, I would like to express my deep gratitude and love to God, Pappa, Mummy, Appacha, Ammachi, Kunju, Mariet, all my friends, and family for their constant support, prayers, and motivation throughout days during my thesis.

List of abbreviations

DLS	Dynamic light scattering
ESA	Excited State Absorption
GSB	Ground State Bleach
IC	Internal Conversion
IRF	Instrument Response Function
ISC	Intersystem crossing
ISMO	Institut des Sciences Moléculaires d'Orsay
ns-TA	Nanosecond Transient Absorption
MEG	Multiple Exciton Generation
PVA	Poly(vinyl)alcohol
QY	Quantum Yield
$[Ru(bpy)_3]^{2+}$	Tris(bipyridine)ruthenium(II)
SBL	Sparse Bayesian Learning algorithm
SE	Stimulated Emission
SEM	Scanning Electron Microscopy
SF	Singlet Fission
SQ	Shockley-Queisser
TA	Transient Absorption
TCSPC	Time Correlated Single Photon Counting
TIPS Anthracene	9,10-Bis[(triisopropylsilyl)ethynyl]anthracene
TIPS Pentacene	6,13-Bis(triisopropylsilylethynyl)pentacene
TIPS Tetracene	5,12-Bis((triisopropylsilyl)ethynyl)tetracene
TTA	Triplet-Triplet Annihilation

Introduction

Singlet Fission and Solar cells

Solar cells are one of the most important renewable and clean energy sources, improvisations to increase the efficiency of photovoltaic conversions can result in revolutionary effects on the world economy, and energy savings and will therefore induce a positive environmental impact. According to the existing Shockley-Queisser (SQ) limit, the maximum efficiency of a single junction solar cell is approximately 34%, primarily because the photon energy exceeding the band gap is lost as heat.(1) In this scenario, an efficient multiple exciton generation (MEG), a process which generates multiple electron-hole pairs after absorption of a photon(2) can be useful to overcome this limit by increasing the external quantum efficiency to 126% and internal quantum efficiency to 200% (2) by reduction of the thermal loss. External Quantum efficiency is the ratio of the number of electrons flowing out of the device to the number of electrons incident on it(3) whereas, Internal Quantum efficiency is the number of electrons collected per absorbed photon(3). Singlet Fission is the most efficient MEG process that can be employed in these cases, which can circumvent the conventional SQ limit(2).

Several studies have been carried out to elucidate the mechanism of singlet fission and to apply it in photovoltaic devices, using high-yielding materials(4). The key to boosting the conversion efficiency of solar cells is to aim for maximum extraction of charge from the low-energy carriers (triplets) and to minimize the parallel loss channels. And hence, studies on the singlet fission molecules gains significant attention.

Basics of Photophysics

When a molecule absorbs light (a photon), it gets converted into energy, consequently, the molecule is promoted from an electronic ground state (S_0) to an excited state (S_1 or S_N). Since this excited state has a high amount of energy, it is deactivated quickly by the photophysical processes (by going back to the ground state) or by the photochemical processes (formation of other species or products).

According to Pauli's Exclusion principle, a maximum of two electrons with opposite spin states (spin pairing) can occupy the same orbital in an atom, and they should not possess the same four quantum numbers (n, l, m_l, and m_s). Singlet state is the state of the molecule when all the electron spins are paired (diamagnetic) and hence does not split in the presence of an external magnetic field. (5). In the excited singlet state (S_1, S_2,..S_N), the excited electron will retain the same spin, and for a triplet excited state, the excited electron will have the opposite spin multiplicity as shown in Fig 1.

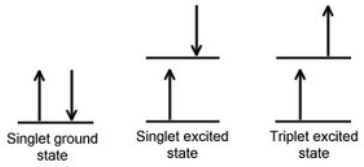

Fig 1. Diagrammatic representation of singlet ground, excited, and triplet excited states.(5)

The name singlet and triplet states, comes from the equation of multiplicity, 2S+1, where S is the total spin angular momentum, which is the sum of spins of all electrons. Individual electron

spins can be s = +1/2 (up spin) or s = -1/2 (down spin). For the singlet excited state, S= 2((+1/2) + (-1/2))+1 = 1 and hence the name singlet. Similarly for the triplet excited state, S= 2((+1/2) + (+1/2))+1 = 3.

The photophysical processes can be best described through the Perrin-Jablonski diagram as given in Fig 2, which details light absorption and the subsequent radiative and non-radiative relaxation processes.

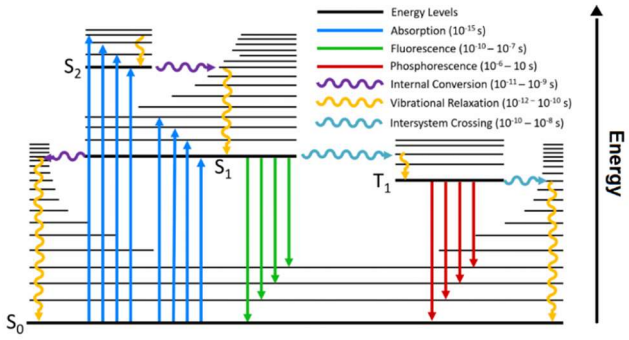

Fig 2. Schematic diagram of Perrin-Jablonski diagram depicting the various processes. The actual processes will occur in faster time scales than the typical timescales in figure(5).

Above mentioned is the Jablonski diagram, which depicts the energy level for the different excited states of an electron. When a molecule in the ground state (S_0), absorbs a photon and goes to the excited state, S_N, it can undergo several deactivation processes – radiative and non-radiative processes. Radiative processes include Fluorescence (emission from the vibronically lowest-lying singlet excited state, according to Kasha's rule) and Phosphorescence (emission from the triplet state). Non-radiative deactivations include Internal conversion (IC) where the transition occurs between two electronic states of the same multiplicity and energy. Vibrational relaxation (VR) is the transition between vibronal levels of the same electronic state and Intersystem crossing (ISC) is the transition occurs between two electronic states of different multiplicity. Apart from these, Triplet-triplet annihilation (TTA) also occurs in certain cases, where two molecules in the triplet state combine to form one molecule in the singlet S_1 state (Figure 3).

$$T_1 + T_1 \rightarrow S_1 + S_0 \qquad \text{(i)}$$

In the case of some molecules, a process opposite to TTA occurs, which is known as Singlet fission (SF), where one singlet (S_1) state splits into two triplets, through a spin-correlated triplet pair intermediate, having an overall singlet character. The process can be endothermic (tetracene, anthracene) or exothermic (pentacene, perylene diimides).

$$S_1 + S_0 \rightarrow {}^1(TT) \rightarrow T_1 + T_1 \qquad \text{(ii)}$$

Extensive studies have been made to understand the singlet fission mechanism and to characterize the intermediate states. Literature (2) suggests that the correlated triplet pair can be formed coherently or incoherently from the singlet excitons. One recent study has proposed that the bound triplet pair ^{1}(TT) state may undergo a spatially separated triplet pair intermediate ^{1}(T⋯T) before it decouples into two independent triplet states.(2) Several mechanisms have been proposed so far which includes the influence of excimer on SF(6), the existence of charge-transfer state(7), formation and dissociation of triplet pairs(8).

Two main factors control the rate of the singlet fission process:

(a) Coupling of the neighboring chromophores:
Molecules in the adjacent chromophores must be in close proximity or should be coupled together to promote singlet fission. (9)

(b) The value of ΔE (10)

$$\Delta E = 2E(T_1) - E(S_1) \lesssim k_B T \quad \text{(iii)}$$

Where k_B is the Boltzmann constant and T is the temperature

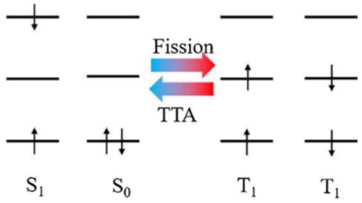

Fig 3. Schematic diagram of Singlet Fission and Triplet-Triplet Annihilation.(11)

Singlet fission is an ultrafast, spin-allowed, down-conversion process by which a high-energy singlet exciton splits to form two low-energy triplet excitons, $E(S_1) \geq 2E(T_1)$ (12), doubling the exciton number in cost of the energy of the singlet. On the other hand, Triplet-Triplet annihilation is an up-conversion process by which two low-energy triplet excitons fuse to form a high-energy singlet exciton, $E(S_1) \leq 2E(T_1)$ doubling the energy in cost of halving the number of excitons (11).

Another process that also generates triplet state as explained in the Jablonski diagram is the Intersystem crossing (ISC), which can be described as the triplet formation from a singlet state through an unimolecular process.(13)

$$S_1 \leftrightarrow T_1 \quad \text{(iv)}$$

ISC is distinguished from singlet fission, as it relies on a single chromophore rather than two, effectively generating one triplet from one singlet exciton and does not involve intermediate states as well as it occurs in a much slower scale (ns) than the singlet fission process (fs-ps) for the acene and rylene families of molecules.

To understand the underlying mechanism behind singlet fission, and to know about the properties of the intermediate states, studies on several acenes have been performed in thin film samples(12,14–18) and in solutions(1,19,20). Unsubstituted acenes usually have relatively low solubility and poor photostability(21), and to improve it, several functional groups have been designed. Of which, the TIPS (triisopropylsilylethynyl) group gains importance, as it enhances the solubility and air stability(22,23) as well as lowers the triplet energy for Pentacene(1).

As above mentioned, the necessity lies in the coupling of the chromophores, whether they had a stacked structure, and hence, studies in nanoparticles suspension of these acenes gained importance and represent a developing field. The nanoparticles are excellent system for these studies because of their solution state, which eases to perform spectroscopic investigations avoiding issues related to thin films such as opacity and localized sample heating. (24) Furthermore, nanoparticles allow to control over the size and morphology of the molecules, and offer the possibility of application in device spin-coating. In this work, we performed preliminary experiments in solutions and nanoparticle solutions of several acenes leading to the singlet fission process, mainly using nanosecond transient absorption spectroscopy.

Materials and Methods

Chemicals: TIPS Pentacene (99%, Sigma Aldrich), TIPS Tetracene (97%, Indagoo), and TIPS Anthracene (99%, BLDpharm) were purchased.

Synthesis of nanoparticle

Taking inspiration from the nanoparticle synthesis reported elsewhere(10), the method of flash precipitation or reprecipitation has been adopted. Under inert (N_2 atmosphere) and dark conditions, 2 mL of sample dissolved in a good solvent (distilled THF) and made into a concentration of 1 mM, is rapidly injected (one step) into 18 mL of vigorously stirred bad solvent (water) or an aqueous solution of PVA (10 ppm). The good solvent should be miscible in the bad solvent. The difference in solubility of the sample solution in THF and water will cause the formation of nanoparticles. 21 gauge disposable needle (Braun 100 Sterican) was used for the rapid injection and the bottles, distilled THF, needles, and syringe, water was degassed for at least 10 minutes before usage. Afterward, the solution is allowed to continue stirring for 30 more minutes to avoid the formation of aggregates. Once, the nanoparticles were formed, the solution was filtered through a 0.22 µm syringe filter (Minisart, Sartorius), to clear the aggregates and was stored in inert and dark conditions. Once, the DLS and nanosecond transient absorption measurements were carried out, the samples were freeze-dried at -63°C at a pressure of 0.02 mbar, for SEM measurements.

THF distillation

Distilled THF has to be used for nanoparticle synthesis since unstabilized THF might have trapped water inside, which will affect the solubility of acenes in it, and hence affect the nanoparticle synthesis. For that, THF distillation was carried out just before each synthesis, which included taking 50 mL of unstabilized THF in a round bottom flask, followed by the addition of 200 mg (2-3 pellets) of benzophenone, a magnetic stirrer, and one plate of Sodium. The latter has to be dried with a tissue and torn into pieces before adding it to the flask. The water bath was placed on a hot plate magnetic stirrer, and adjusted to the required height. A distillation tube was attached to the round bottom flask, maintaining an N_2 flowing atmosphere through one of the valves and water connection along the condenser. THF boils at 60°C, the stirrer is kept at 500 rpm, and the temperature is set to 80°C. Once the Sodium absorbs the water and benzophenone turns blue, the temperature was set to 90°C, and the water is allowed to flow through the condenser, allowing the THF to distillate and be collected in the receiver flask.

PVA stock solution

The synthesis for the stock solution of PVA has been reported elsewhere (24), where 1000 ppm stock solution of PVA (MW: 130-150 kg/mol, 86.7-88.7% degree of hydrolysis, Sigma Aldrich), was prepared by weighing 50 mg of PVA and adding slowly into 50 mL of stirred distilled water. The solution is allowed to stir for another 2 hours at a temperature of 90°C.

Dynamic light scattering

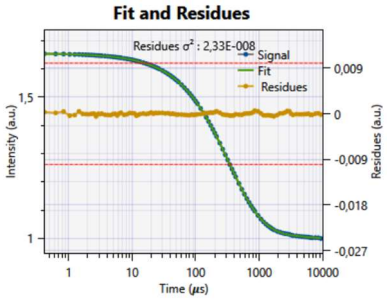

Real-time/time-resolved nanoparticle size measurements were made using VASCO KIN, with Nanokin software, (Cordouan technologies). 635 nm wavelength, 50 mW power - High stability laser diode was used for the measurements. For each measurement, the alignment of the Laser and the correlogram, fit/residues were thoroughly checked, repetitions were made wherever necessary, and the hydrodynamic size of the freshly prepared nanoparticle solution was measured. SBL is based on an iterative algorithm for particle size distribution calculations. SBL measurements having a good correlogram and fit as given in the figure on the right, were taken to estimate the size of the nanoparticles. 1cm*1 cm cuvettes were used for DLS measurements.

Scanning electron microscopy

SEM measurements were carried out in Ziess 1540 type scanning electron microscope (resolution of 1.1 nm at 20kV to 2.5 nm at 1 kV), to understand the morphology and size of the synthesized nanoparticles. The freeze-dried nanoparticles were placed on a carbon holder, making thin films by spin coating, for which 2.5 nm Plasma was added to the top of the dried sample in Argon atmosphere, followed by the addition of a layer of 3 nm of gold (sputtering-to provide conductivity). The images were analyzed using Image J for size measurements.

Steady-state absorption and emission

The steady-state absorption measurements were performed in the Cary 300 UV Win (Agilent technologies) spectrophotometer. The emission measurements were performed using a Cary Eclipse fluorimeter. Emission measurements were performed by exciting the sample, with an absorbance of less than 0.1. For hard sphere measurements, a QuantaPhi2 (Horiba scientific) spectrophotometer with a PLQY integrating sphere was used.

Time-correlated single photon counting (TCSPC)

The TCSPC measurements were carried out using the PicoHarp 300 TCSPC system (time bin=4ps). Fluofit Picoquant software was used to analyze the emission decay which was treated with a weighted sum of exponential decays convolved by IRF signal measured using a scattering Ludox solution (prompt). Solutions with absorbance less than 0.1 at excitation wavelength were used for the measurements.

Nanosecond Transient absorption

The transient absorption spectroscopy is used to probe the dynamics of transient species in an excited state or in a photochemical reaction. A pump (excitation) pulse promotes a fraction of molecules to an electronically excited state, while a probe pulse, which is a white light continuum, generally of low intensity, is sent to measure the absorption of the sample at a delay time τ with respect to the pump pulse. Due to the difference between the absorption of the excited state and the ground state molecule, a differential absorption spectrum of $\Delta A(\lambda,\tau)$ or the transient absorption spectrum is obtained. The transient absorption (TA) spectrum can give information on the signature and evolution of transient species involved at different wavelengths. For example, excited singlet and triplet states, electron and energy transfer processes or photo-product reactions can be observed. The ΔA profile obtained by the transient absorption spectra can be expressed by the equation given below:

$$\Delta A = \log_{10}\left(\frac{s^{p}_{ref}}{s^{0}_{ref}} X \frac{s^{0}_{sample}}{s^{p}_{sample}}\right) \quad \text{(iv)}$$

where ΔA is difference absorption, s^{p}_{ref} and s^{0}_{ref} are reference spectra with and without pump, respectively, while s^{p}_{sample} and s^{0}_{sample} are sample spectra with and without pump.

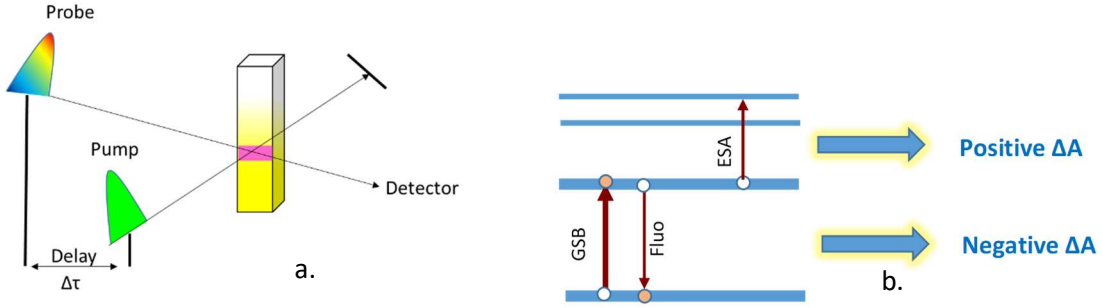

Fig. 4 (a) A general representation of a TA set-up showing the pump pulse photoexciting the sample and the probe pulse monitoring the sample response at different delay times after photoexcitation and (b) contributions in a ΔA spectrum.

Process	ΔA	Reason
Ground state bleaching (GSB)	negative	Excitation of the molecule results in a decreased absorption of the excited state molecule than the non-excited molecules
Stimulated emission (SE)	negative	Emission from the excited molecules induced by the probe pulse.
Excited state absorption (ESA)	positive	Promotion of excited state population to higher excited state by the probe beam.

Table 1. Different processes in transient absorption spectra.

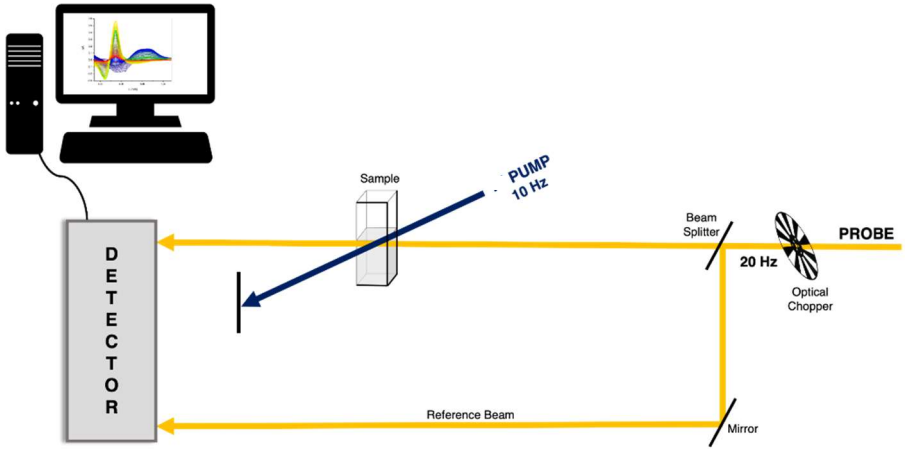

Fig 5. Schematic diagram of nanosecond transient absorption set up.

The nanosecond transient absorption set up in ISMO has EKSPLA (Nd: YAG laser head) with OPO (Optical Parametric Oscillator) tunable (410 nm-NIR) pump laser which operates at 10 Hz. The probe laser LEUKOS, is a supercontinuum laser that operates at 2kHz repetition rate and is reduced using a chopper to 20 Hz. The probe beam passes through a beam splitter to

generate a reference beam, which accounts for the laser fluctuations and noises. Detection is carried out using the spectrograph (SPX-270M Jobin-Yvon) coupled to intensified CCD (PIMAX 4, Princeton instrument).

Results and Discussions

4.1. TIPS Pentacene in THF

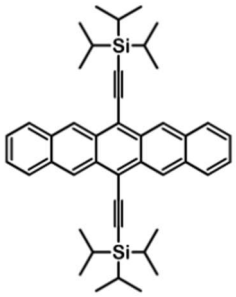

Fig 6.Structure of 6,13-bis(triisopropylsilylethynyl)pentacene

To start with, we performed the photophysical studies of TIPS Pentacene in THF (Molar absorption coefficient at 590 nm = 22200 $M^{-1}cm^{-1}$) (1) with a concentration of 0.01 mM.

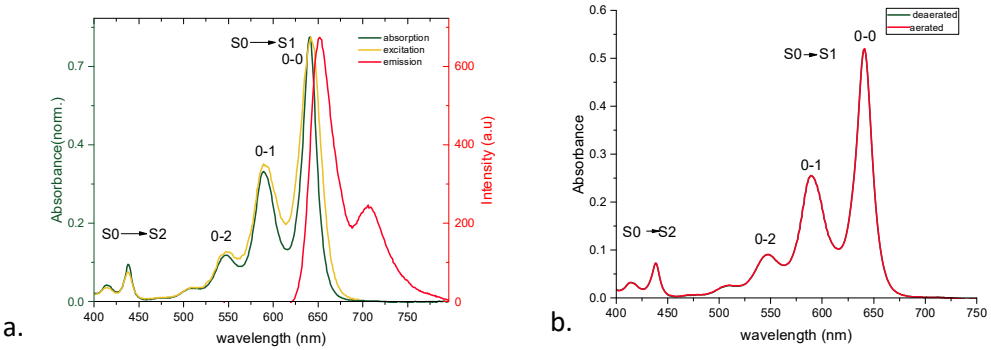

Fig 7. (a) UV−visible absorption, excitation ($\lambda_{emission}$ = 706 nm) and fluorescence spectra ($\lambda_{excitation}$ = 539 nm) of TIPS Pentacene in THF (0.01 mM), measured in 1 cm cuvette. (b) UV-vis absorption spectrum of deaerated and aerated solution.

The UV-Vis absorption spectrum shows the peaks at 645 nm, 595 nm, 550 nm, corresponding to the $S_0 \rightarrow S_1$ vibronic transitions 0-0, 0-1 and 0-2 respectively and a peak at 440 nm corresponding to the $S_0 \rightarrow S_2$ transition. The spectra also shows the overlap of absorption and excitation spectra of TIPS Pentacene solution in THF, as well as the Stokes-shifted emission spectrum, with an emission maxima at 647 nm and 703 nm from the two $S_1 \rightarrow S_0$ vibronic transitions 0-1 and 0-0 respectively.

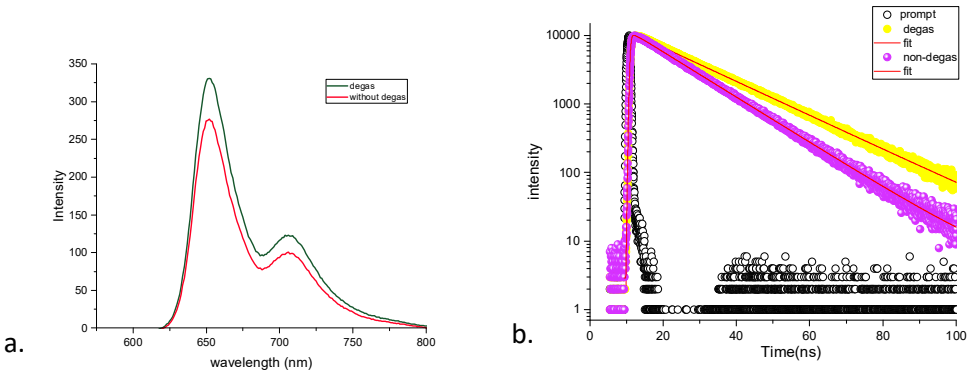

Fig. 8. (a) Comparison of fluorescence spectra ($\lambda_{excitation}$=539 nm) of TIPS Pentacene in THF (0.05 mM), measured in 1 cm cuvette in deaerated (green) and aerated condition (red). (b) Comparison of decays obtained by TCSPC of degassed (yellow) and non-degassed (pink) solutions of TIPS Pentacene in THF, excited at 483 nm (OD=0.05).

An increase in the emission intensity is observed in aerated solution; however, the spectral shape is similar in both conditions. Since the emission (fluorescence) spectra correspond to the relaxation from the S_1 lowest-lying state (according to Kasha's rule), this decreased emission intensity in the presence of oxygen reveals additional non-radiative relaxation pathways in the presence of oxygen.

As observed from the TCSPC results, the presence of oxygen causes a faster decay of the singlet state compared to the sample without oxygen. The mono-exponential lifetimes obtained are listed in table 2. The deaerated solutions exhibited a shorter singlet state lifetime than the aerated solution, which can be attributed to the oxygen-catalyzed singlet fission process as previously observed by Wollscheid et al.(1).

TA (Transient absorption) data analysis

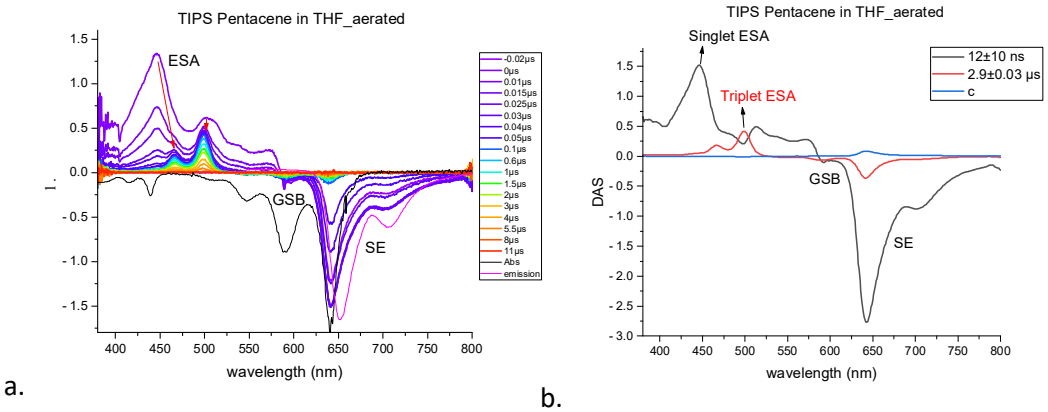

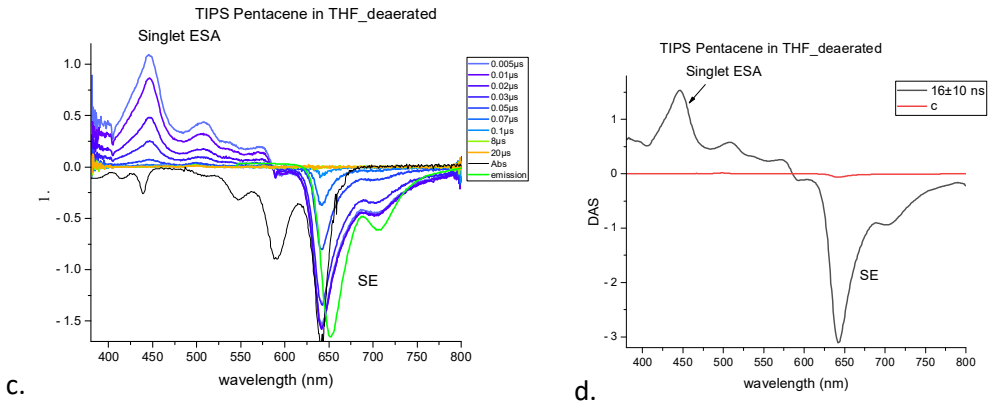

Fig 9. (a) Transient absorption spectra of deaerated TIPS Pentacene solution (0.02 mM) (b) Decay associated spectra obtained after fitting and (c) Transient absorption spectra of aerated TIPS Pentacene solution in THF and (d) Decay associated spectra of the aerated solution obtained after fitting exciting at 638 nm (OD = 0.45), 1 cm cuvette.

The effect of oxygen on the dynamics of excited state of TIPS pentacene was also investigated using nanosecond transient absorption. In aerated conditions, singlet excited state absorption (ESA) features are observed at 446 nm and 500 nm, which followed by the signature of triplet state ESA at 468 nm and 500 nm from 25 ns, as denoted by the red arrows in Fig (9a). The ground state bleaching (GSB) at 596 nm and 641 nm corresponded to $S_0 \rightarrow S_1$ vibronic transitions 0-0, and 0-1 respectively. Emission bands are observed at 642 nm and 705 nm. This is confirmed by the overlap of steady-state absorption and emission spectra with the transient spectra. Global fit was applied to the TA spectra, resulting in a bi-exponential functions with lifetimes of $\tau1$=12±10 ns and $\tau2$= 2.9±0.1 µs, corresponding to singlet and triplet lifetimes ,respectively, as confirmed by both their signature and lifetimes reported in the literature(1).

For the deaerated solution, similar transient signature of singlet state is observed. Kinetic traces were fitted mono-exponentially with a lifetime of $\tau1$=16±10 ns, corresponding to the singlet lifetime. However, no signature of triplet excited state was detected.

These observations of deaerated and aerated solutions of TIPS Pentacene in THF provide some interesting insights. Under aerated conditions, where oxygen is present, the triplet state is typically quenched. However, we observe contrary results indicating the oxygen-catalyzed singlet fission as reported by Wollscheid et al(1).

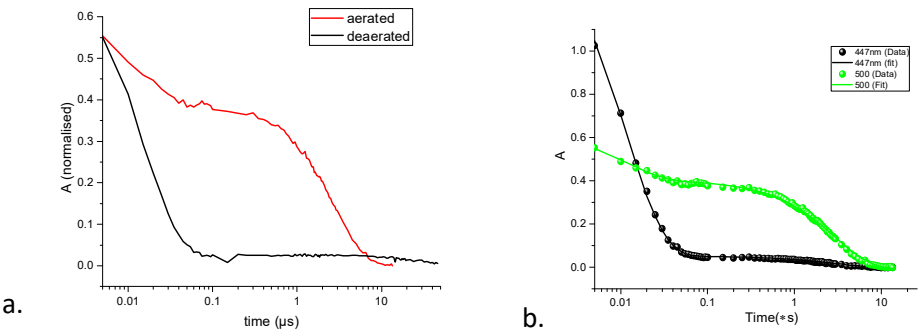

Fig 10. Comparison of decays at 500 nm between the deaerated (black) and aerated (red) solutions of TIPS Pentacene in THF obtained from ns TA. (b). Fitting of decays at 447 nm (singlet) and 500 nm (triplet) for deaerated solution of TIPS Pentacene in THF.

The decays does not depend on the power for TIPS Pentacene solution in THF.

Fig 10 confirm the presence of triplet state in deaerated conditions with microsecond decay times and the absence of triplet state in aerated condition. Wollscheid et al (1) suggested the oxygen catalyzed sequential singlet fission in TIPS Pentacene solutions, where two triplets are generated by exploiting $^3O_2$ as a catalyst. The schematic diagram of the oxygen-catalyzed singlet fission is shown below:

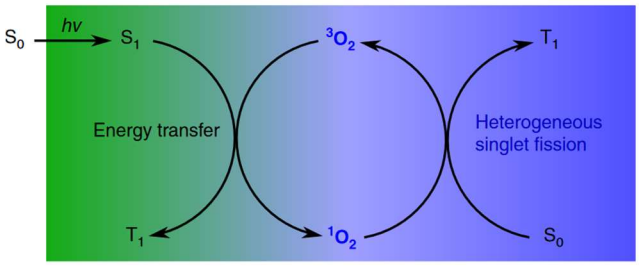

Fig 11. Schematic diagram of oxygen-catalysed singlet fission in aerated TIPS Pentacene solution in THF.(1)

Wollscheid et al (1) proposed this to occur in two steps:

(a) Upon excitation of the acene to its S_1 by absorption of a photon, it transfers the energy to $^3O_2$ to yield a triplet acene T_1 and $^1O_2$.
(b) The produced $^1O_2$ combines with another ground state acene (S_0), forming the second triplet excited state of the acene and regenerating the $^3O_2$, thereby acting as a catalyst. Having a condition of

$$E(S_1) - E(T_1) \geq E(\ ^3O_2\ ) = 0.977\ eV \qquad \text{(iii)}$$

Along with the Energy of ($S_1 - T_1$) ≥ Energy of ($^1O_2 - {}^3O_2$), so that the singlet excited state can transfer energy to the $^3O_2$ and the Energy of ($T_1 - S_0$) ≤ Energy of ($^1O_2 - {}^3O_2$) for the energy transfer from $^1O_2$ to the ground state molecule(1).
The quantum yield of this energy transfer can be calculated using the equation below:

$$QY = \frac{k_1[\ ^3O_2]}{k_{tot}} \qquad \text{(v)}$$

Where, the rate of energy transfer, $k_1 = 3.12 \times 10^{10}$ $(Ms)^{-1}$ (1) for atmospheric conditions with an $[^3O_2]$=1.81 mM, as given in the literature(1) and $k_{tot} = \frac{1}{t_1}$.
A quantum yield of 67.8% is obtained for the oxygen-catalyzed singlet fission.

TIPS Pentacene	Lifetime (ns)	
	TCSPC	**ns TA**
Aerated	**τ1=13.1±0.01 ns**	**τ1=12±10 ns**
Deaerated	**τ1=17.5±0.01 ns**	**τ1=16±10 ns**

Table 2. Lifetimes of aerated and deaerated solutions of TIPS Pentacene in THF, obtained through TCSPC and nsTA measurements..

4.2. TIPS Pentacene nanoparticle

Nanoparticles of TIPS Pentacene was prepared through flash-precipitation as mentioned in the materials and methods section. Extensive studies have shown that Pentacene systems undergo slightly exergonic singlet fission, which occurs within the 100fs of excitation (24).

Two type of nanoparticles were synthesized from a 1 mM stock solution in distilled THF in deaerated and dark conditions:

(i) 2 mL of TIPS Pentacene in THF added to 18 mL water (60 ppm TIPS Pentacene).
(ii) 2 mL of TIPS Pentacene in THF added to a solution of 0.64 mL PVA and 17.4 mL water (60 ppm TIPS Pentacene/30 ppm PVA)

Both types resulted in the formation of blue-colored nanoparticle solution.

a. 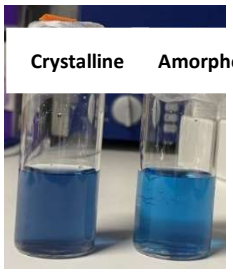

b. 

Fig 12. (a) Crystalline and amorphous nanoparticles of TIPS Pentacene in aqueous PVA and in water respectively. (b) Syringe used for experiment (left) and syringe with the Silicon-containing polymer at the stopper (right).

PVA (Poly(vinyl) alcohol) is a polymer, commonly employed in nanoparticle dispersions as emulsifying or capping agents to promote particle dispersity and minimize aggregation(24). The UV-vis spectra obtained have been plotted in Fig 13(a). Initially, the freshly prepared nanoparticle samples of both types had the same shape and peaks. By the second day, as shown in Fig 13(b), a new peak started to form at 700 nm for TIPS Pentacene nanoparticle with PVA, which shows the formation of crystalline domains in the nanoparticle solution(24). Hudson et.al(24) added Polyethylene glycol and Stuart et.al (25) used Polymethylmethacrylate as an additive and didn't observe the crystalline behavior. Hence, this behavior is induced only by PVA addition and can be attributed to the dispersion-dipole forces between the polar OH groups of PVA and non-polar isopropyl groups of TIPS-Pentacene(24). It is also likely that the molecular displacement between adjacent, slip-stacked molecules in the crystal have nearly 3 times the interhydroxyl spacing of PVA (3*2.520=7.560 Å)(24), this regular periodicity can contribute to stabilizing the crystalline morphology of these nanoparticles.

A similar effect is observed when using the BD Syringe (Fig 12.(b)) to introduce TIPS Pentacene stock solution in THF into the water during synthesis. It has been later confirmed that the presence of an unknown silicon-containing polymer (26) at the end of the syringe stopper induces this effect. However, the solution formed in this protocol degrades over time and prompting the use of PVA solution to achieve a more stable solution.

The absorption change in crystalline form is attributed to the Davydov splitting of the 0-0 vibrational band of the $S_0 \rightarrow S_1$ peak. Davydov splitting arises from the strong overlap of the two translationally non-equivalent molecules in the unit cells of crystals(27). This has been reported for polycrystalline crystal samples (28), pentacene dimers (27), acene films (17), and nanoaggregates (10) and has been predicted to have a charge-transfer mediated character that supports singlet fission(27), particularly in pentacene single crystals where singlet fission occurs rapidly. In short, Davydov splitting can be used as a parameter to distinguish different kinds of excimers and their roles, and its nature depends on the electronic interaction between the neighboring molecules in the ground state rather than the excimer states, where the interaction is solely based on the electronically excited state of the two adjacent chromophores.

(29) Therefore, the Davydov splitting reported is found to induce a strong intermolecular π- π interaction, which leads to intermolecular coupling and hence leads to Davydov splitting. (27)

Apart from these, notable visual changes are observed when the nanoparticles in the PVA solution are aged over time, as the new peak arises, the clear blue colored nanoparticles change to a greyish-blue color as given in Fig 12(a).

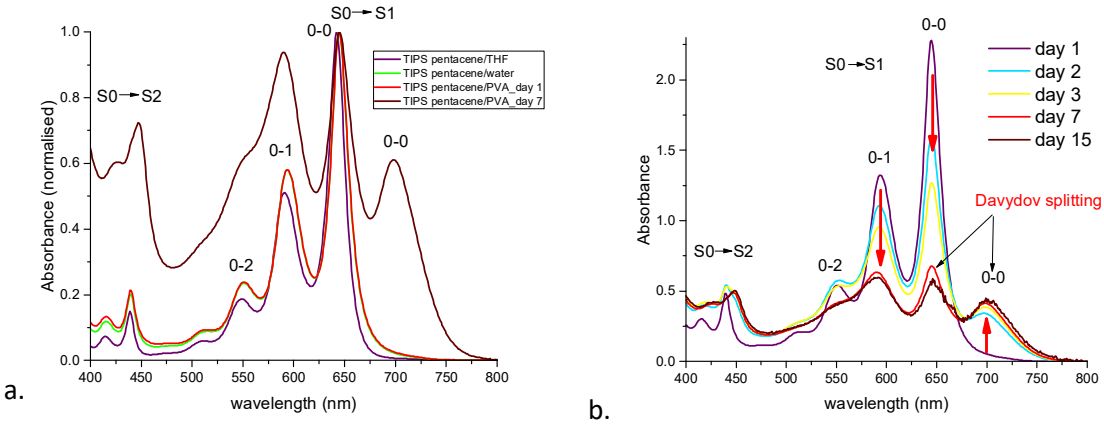

Fig 13. (a) Normalised UV−visible absorption spectrum of TIPS Pentacene in THF (violet), TIPS Pentacene nanoparticle in water (green), TIPS Pentacene nanoparticle in aqueous PVA-day 1 (red) and TIPS Pentacene nanoparticle in aqueous PVA- day 7, (b). Control of UV-visible spectra of TIPS Pentacene nanoparticle in aqueous PVA until day 15.

In fig 13(a), the increase in absorbance at 400 nm compared to the solution in THF for the nanoparticle solutions represents the scattering induced by the nanoparticles when and hence it confirms the formation of nanoparticles as well. Moreover, the nanoparticle solutions have a slightly red-shifted spectrum in comparison with the solution which is attributed to the solvatochromic effects as reported by Pensack et al., 2015(30). The slight change in relative vibronic intensity for nanoparticle and solution has been assigned to the weak intermolecular coupling of the nanoparticle solution(30). The PVA chains induced large-scale reorganization of TIPS Pentacene molecules 24 hours after synthesis when kept at 5°C, which opposes to the changes observed by Hudson et.al(24) in several minutes.

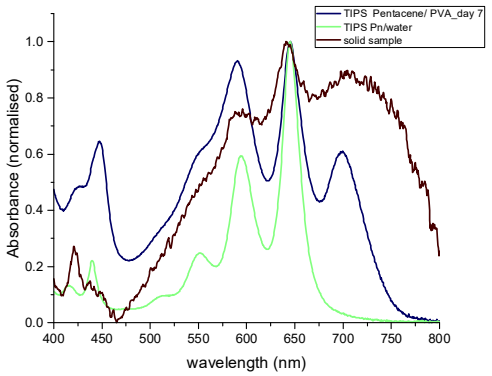

Fig 14. UV-Visible spectra of crystalline TIPS Pentacene nanoparticle (blue), amorphous TIPS Pentacene nanoparticle (green) and solid sample of TIPS Pentacene powder (brown), measured using integrating sphere.

To confirm the crystallinity of the nanoparticle sample with PVA, solid state UV-vis absorption spectra were performed for the pristine TIPS Pentacene powder available commercially, using an integrating sphere and $BaSO_4$ as a solid state solvent. The results obtained depicted in fig 14, show the presence of the peak at 700 nm, which is also observed in the pristine powder of TIPS Pentacene, confirming the crystallinity of the nanoparticle sample made with PVA. Hence from here onwards, we will refer to the nanoparticles made in aqueous PVA solution as 'crystalline' nanoparticles and those made in water to be 'amorphous'. This is also confirmed by characteristic X-ray reflecting due to its sufficient structural order for the sample containing PVA, confirming its long-range order when compared to the amorphous nanoparticle, which has short-range order as reported by Hudson et.al(24).

Days	Percent crystallinity
Day 15	72
Day 7	67
Day 3	41
Day 2	29
Day 1	4

Table 3: The relative measure of percentage crystallinity was determined using the ratio of absorbance at 700 nm to 645 nm, this method is adopted from Tayebjee et.al(10).

Dynamic light scattering (DLS) gives information on the hydrodynamic size of the synthesized nanoparticles. The crystalline sample of TIPS Pentacene was monitored for 15 days until complete crystallization was achieved. Each time a 0.22 µm syringe filter was used to remove larger nanoparticles. The results show that as the crystallinity of the nanoparticle sample increases, a new population of smaller-sized nanoparticles forms, the size (in nm) have been tabulated in Table 4 below. This shift to smaller size as the crystallinity increases, can be due to the tendency to minimize the nonfavorable nanoparticle-solvent interactions, nanoparticles tend to form small clusters, which act as nuclei to initiate crystallization, aided by the increased stacking between the molecules in crystalline nanoparticles. This increased interaction between the molecules in the nanoparticle, leads to desorption of adsorbed polymer from the nanoparticle surface and hence a decrease in particle size(31).

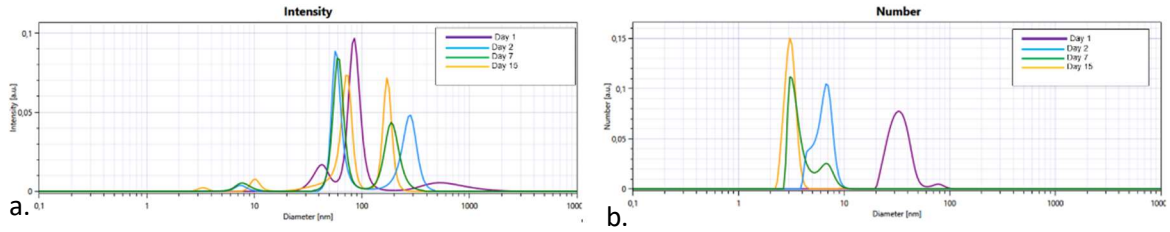

Fig 15. DLS results of crystalline TIPS Pentacene nanoparticle over a span of 15 days, (a) SBL intensity, (b) SBL number.

TIPS Pentacene	SBL intensity (nm)	SBL number (nm)
Day 1	43,85,543	32,78
Day 2	7,56,284	7
Day 7	7,59,187	3,7
Day 15	3,10,71,171	3

Table 4. Size of nanoparticles obtained from DLS measurements over a span of 15 days for crystalline TIPS Pentacene nanoparticles.

Amorphous vs crystalline nanoparticle of TIPS Pentacene

A comparison of the size of the amorphous and the crystalline nanoparticles reveals the decrease in size when the particles are forming crystalline structures. This can be due to the increased intermolecular coupling between the adjacent chromophores in the crystalline nanoparticles resulting in smaller sizes. On the first day, the solution with PVA had a higher hydrodynamic size due to the polymer adsorption onto the nanoparticle surface, which decreases as the crystallinity of the sample decreases.

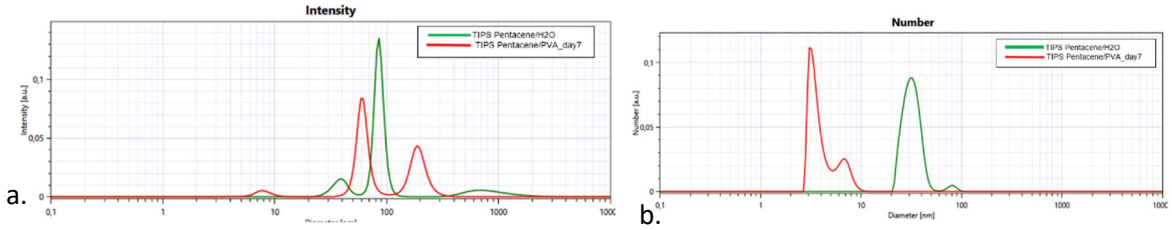

Fig 16. DLS results of comparison of amorphous and crystalline nanoparticles of TIPS Pentacene, (a) SBL intensity and (b) SBL number.

TIPS Pentacene	SBL intensity (nm)	SBL number (nm)
Amorphous	39,85,684	31,83
crystalline	7,59,187	3,7

Table 5. Size of nanoparticles obtained from DLS measurements for amorphous and crystalline nanoparticles of TIPS Pentacene.

TA data analysis:

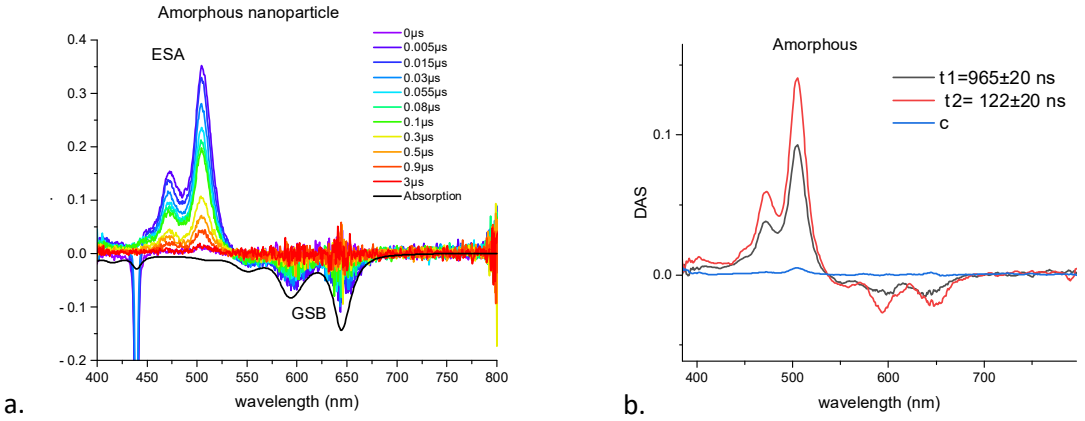

Fig 17. (a)Transient absorption results of amorphous TIPS Pentacene nanoparticle (b) Decay associated spectra of the deaerated solution obtained after exciting at 440 nm (OD=0.5), power 15 mW, 1 cm cuvette.

From the transient absorption spectra in fig 17(a), the ground state bleach feature is observed at 553,594 and 645 nm, corresponding to the ground state absorption spectra of $S_0 \rightarrow S_1$ vibrational transitions of 0-2, 0-1, and 0-0, respectively. The spectra have intense ESA features at 472 and 500 nm, which corresponds to triplet excited states ($T_1 \rightarrow T_N$ transition) and the shape of the spectra remains the same throughout.

The decays at the 472 nm and 500 nm are identical. A global fit is used to fit the TA spectra, yielding two lifetimes $\tau1$=965±20 ns and $\tau2$= 122±20 ns for triplet states of two nanoparticle populations for amorphous TIPS Pentacene.

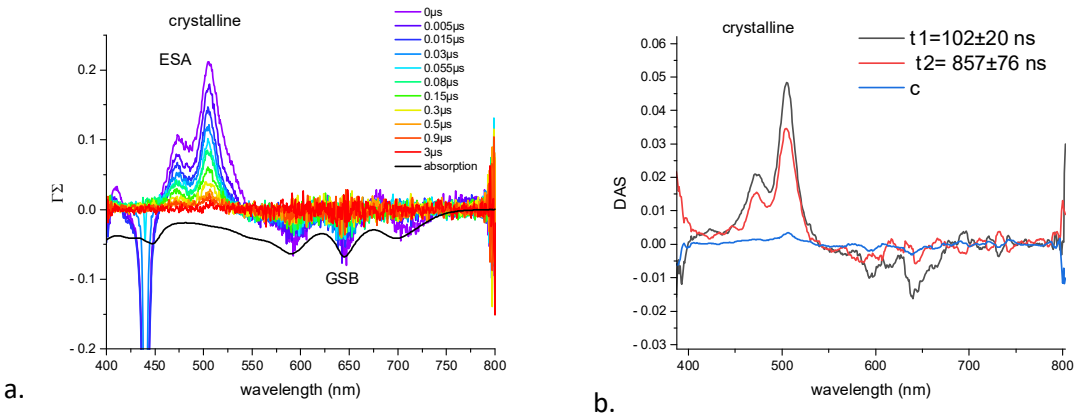

Fig 18. (a)Transient absorption results of crystalline TIPS Pentacene nanoparticle having a 7 days of age (b) Decay associated spectra of the deaerated solution obtained after exciting at 440 nm (OD=0.5), power 15 mW,1 cm cuvette.

In case of crystalline nanoparticles (fig 18 (a)), global analysis is used to fit the TA spectra and two lifetimes τ1=102±20 ns and τ2= 857±76 ns are obtained for triplet states of two nanoparticle populations. The zero time spectra of crystalline nanoparticles have a different shape in comparison with the amorphous. Hudson et. al(24) reported that the singlet fission gets accelerated in crystalline TIPS Pentacene nanoparticles by an order of magnitude due to the structural rearrangement.

Morphological analysis of the crystalline TIPS Pentacene nanoparticle has been conducted using SEM measurements. The particles were cubical and had a size of 0.552±0.2 μm, upon statistical analysis using Image J software. The size distribution obtained has been plotted in a histogram as shown below in Fig. 19 (b). The morphology of nanoparticles reveals a diffused layer of PVA coating on the surface of the nanoparticles.

Freeze-dried particles were used for SEM characterization, since the solvent for nanoparticle solution was water, and the electron beam requires vaccum for detection, moreover presence of water can also damage the microscope(32). Hence, the change in physical state might have caused the slight increase in their size as compared to the DLS results, where the size was measured in solution state. As well as, the DLS measurement assumes particles to be spherical in shape(33), whereas the nanoparticles have a cubical shape as observed through SEM, and hence difference in particle size is observed.

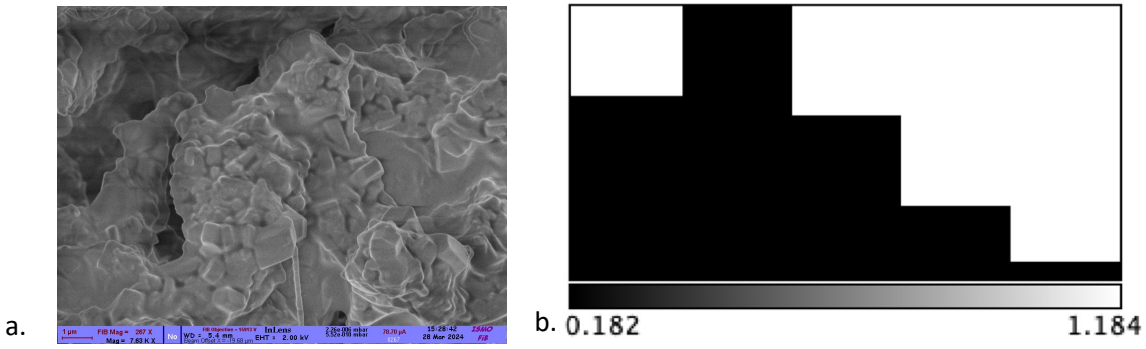

Fig 19. (a) SEM measurements of crystalline TIPS Pentacene nanoparticles, (b) Histogram of size distribution in μm scale.

Triplet yield calculation:

The triplet quantum yield was quantified using relative actinometry using the aqueous solution of $[Ru(bpy)_3]^{2+}$ as a reference. The intensity of the transient absorption changes on decreasing the laser power intensity of the pump was recorded for both the reference and the nanoparticle solution of TIPS Pentacene under the same experimental conditions ($\lambda_{excitation}$, pathlength, absorbance at the excitation wavelength).

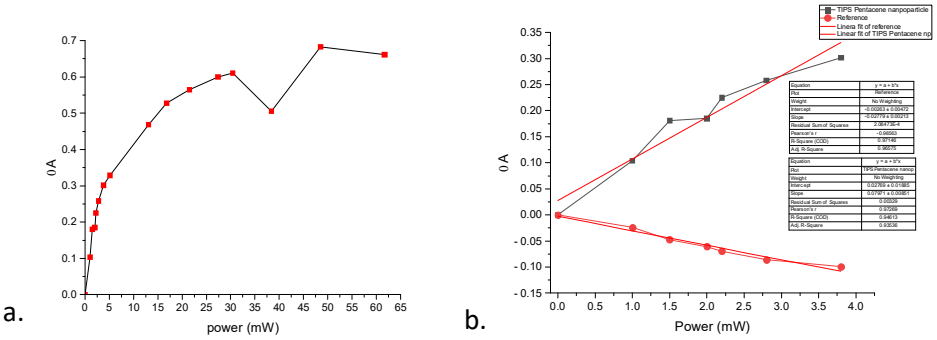

Fig 20. (a) Plot of ΔA vs excitation power (saturation curve) for TIPS Pentacene nanoparticle solution, at $\lambda_{excitaion}$ = 440 nm, OD= 0.4 at 440nm, path length 1 cm. (b) Plot of A vs excitation power for $[Ru(bpy)_3]^{2+}$ in red, 455 nm and for TIPS Pentacene nanoparticle in black, 505 nm, $\lambda_{excitaion}$ 440 nm, OD= 0.4 at 440nm, path length 1 cm.

From the saturation curve, the linear region of the power was found for TIPS Pentacene nanoparticle and the $[Ru(bpy)_3]^{2+}$. By using the values of the slopes obtained by linear regression of TIPS Pentacene nanoparticle and the reference in equation, the triplet quantum yields were obtained.

$$\varphi_T = \frac{slope_T \times \varphi_{ref} \times \Delta\varepsilon_{ref}}{slope_{ref} \times \Delta\varepsilon_T}$$

Where φ_T is the triplet quantum yield to be calculated, $\Delta\varepsilon_T$ is the triplet molar extinction coefficient of TIPS Pentacene at 505 nm $\Delta\varepsilon_T$ = 98600 $M^{-1}cm^{-1}$ (34). φ_{ref} is the quantum yield of $[Ru(bpy)_3]^{2+}$ ($\varphi_{ref}\approx 1$) and $\Delta\varepsilon_{ref}$ is the absolute value of molar absorption coefficient for the $[Ru(bpy)_3]^{2+}$ reference ground state bleach at 455 nm = -10100 M^{-1} cm^{-1}(35).

Triplet QY for TIPS Pentacene nanoparticle was determined to be 31.4%

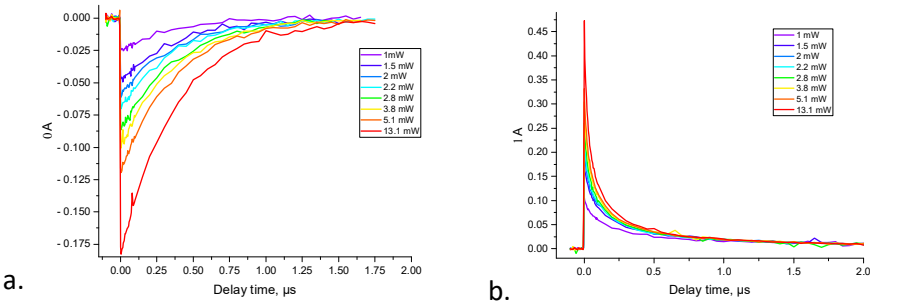

Fig 21.Transient absorption decays recorded at varying powers of excitation pulse $\lambda_{excitaion}$ = 440 nm for (a) $[Ru(bpy)_3]^{2+}$ in water recorded at 455 nm, (b). TIPS Pentacene nanoparticle at 505 nm.

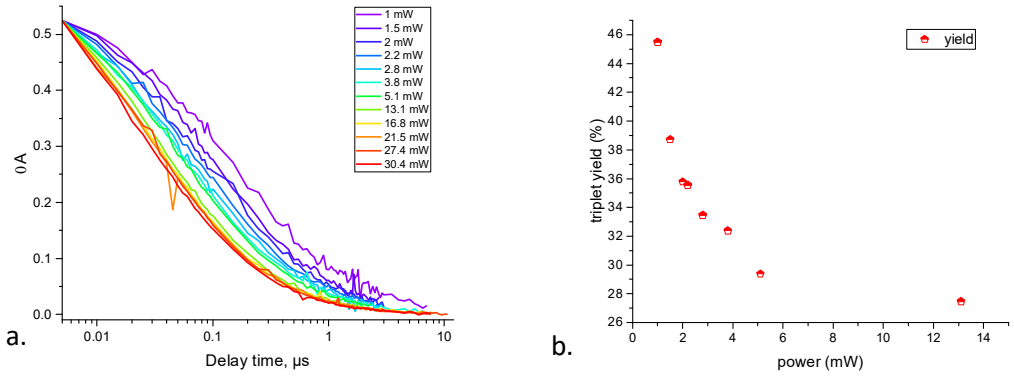

Fig 22. (a) Normalized decays of TIPS Pentacene nanoparticle solution at different excitation powers, when excited at 440 nm. (b) A plot of percentage triplet yield vs power for TIPS Pentacene nanoparticle solution.

The decays were independent of the excitation power of the laser for the TIPS Pentacene in THF, on the contrary, the decays are dependent on the excitation power for the TIPS Pentacene nanoparticle as seen in Fig 22(a). This power dependency can be due to the possibility of the triplet exciton annihilation(26) or singlet-singlet annihilation(36) process occurring in the nanoparticle solution.

As observed in Fig 22(a), faster decays are observed for higher powers. When we calculated the triplet yield at each power as given in Fig 22(b), the yield decreased for higher laser power. This trend along with the saturation tendency of excitation intensity on the amount of T_1 state as plotted in Fig 20(a), suggests the possibility of singlet-singlet annihilation process along with the singlet fission process. Singlet-singlet annihilation is the process by which there is a generation of higher excited singlet states (S_N) from two excited singlet molecules.

$$S_1 + S_1 \rightarrow S_N + S_0 \qquad \text{(i)}$$

This S_N molecule can generate the two triplets via singlet fission, and hence two singlet excited state molecules are used to generate two triplet excited states. Thereby a decrease in the triplet yield is observed when the singlet-singlet annihilation process occurs along with singlet fission.(36). This process needs to be confirmed with femtosecond experiments, nevertheless from our nanosecond experiments, the triplet excitation population in the nanoparticles is highly sensitive to incident pump intensity.

4.3. TIPS Tetracene in solution

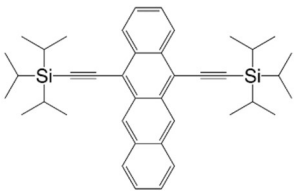

Fig 23. Structure of 5,12-bis((triisopropylsilyl)ethynyl)tetracene

Studies were done in TIPS Tetracene in THF (Molar absorption coefficient at 515 nm=24000 $M^{-1}cm^{-1}$) (37) solution with a concentration of 0.08 mM.

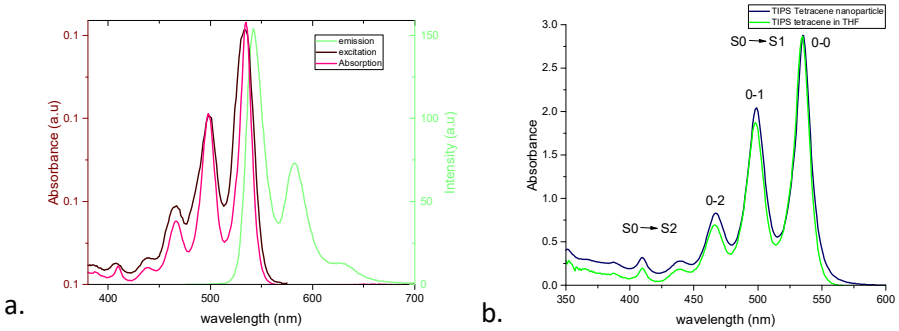

Fig 24. (a) UV−visible absorption, excitation ($\lambda_{emission}$ = 582 nm) and fluorescence spectra ($\lambda_{excitation}$ = 466 nm) of TIPS Tetracene in THF(0.08 mM), measured in 1 cm cuvette. (b) UV-vis absorption spectrum of TIPS Tetracene in THF (green) and TIPS Tetracene nanoparticle (blue).

The absorption, excitation and emission spectra of TIPS Tetracene in THF are given in Fig 24(a). The emission spectrum is the mirror image of the absorption spectrum and the excitation spectrum overlaps with the absorption spectrum. The characteristic peaks have been assigned from the literature(38) as : $S_0 \rightarrow S_1$ transitions at 536 nm, 500 nm, 467 nm corresponding to 0-0, 0-1 and 0-2 vibronic transitions, respectively, and $S_0 \rightarrow S_2$ transition at 411 nm. The emission features had three peaks at 542 nm, 582 nm and 628 nm corresponding to $S_1 \rightarrow S_0$ 0-0, 0-1, and 0-2 vibronic transitions respectively.

TA data analysis:

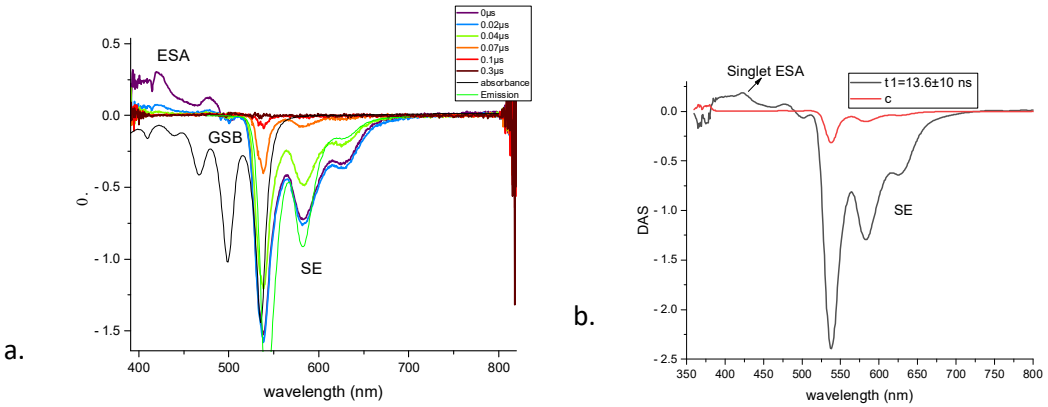

Fig 25. (a)Transient absorption results of deaerated TIPS Tetracene solution (0.08 mM) in THF (b) Decay associated spectra obtained after fitting, excited at 491nm, absorbance=0.4, power 0.7 mW, 1cm cuvette.

From the transient absorption spectra in fig 25(a), the Ground state bleach feature is observed at 500 and 536 nm, which follows the Ground state absorption spectra and corresponds to $S_0 \rightarrow S_1$ 0-1 and 0-0 vibronic transitions, respectively. The solution of TIPS Tetracene is highly emissive in nature and hence low excitation pump powers were required to get spectra without having emission saturation. The stimulated emission features are observed at 536 nm, 582 nm and 628 nm, with the GSB and SE almost overlapped at the 536 nm. The spectra has ESA features at 415 and 470 nm, which corresponds to singlet excited states ($S_1 \rightarrow S_N$ transition) which decays rapidly. Triplet states are not essentially visible in the solution. A global fit is used to fit the TA and obtained $\tau 1 = 13.6 \pm 10$ ns for the singlet state.

4.4. TIPS Tetracene nanoparticle

Nanoparticles of TIPS Tetracene was prepared through flash-precipitation as mentioned in the materials and methods section. Extensive studies have been made on Tetracene systems and it is found to undergo a slightly endergonic singlet fission, which occurs within the 200ps of excitation(2).

Nanoparticles were synthesized from a 1 mM stock solution in distilled THF in deaerated and dark conditions.

2 mL of stock solution was added to vigorously stirred 18 mL of distilled water, which lead to the formation of pinkish orange-coloured nanoparticles.

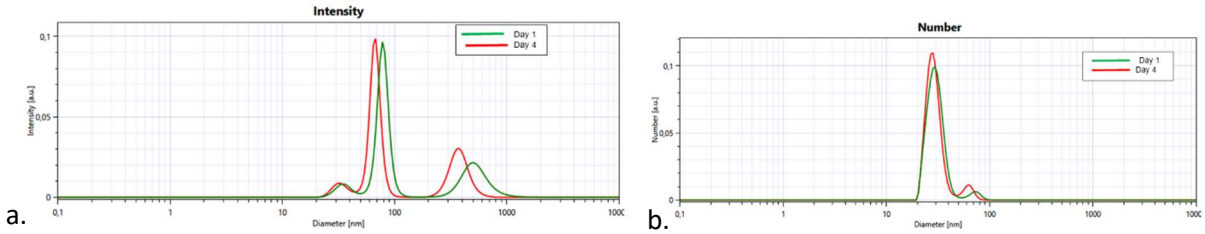

Fig 26. DLS results of TIPS Tetracene nanoparticle over a span of 4 days, (a) SBL intensity, (b).SBL number.

TIPS Tetracene	SBL intensity (nm)	SBL number (nm)
Day 1	35, 78, 495	29, 74
Day 4	32, 68, 375	28, 62

Table 6. Size of nanoparticles obtained from DLS measurements over a span of 4 days for TIPS Tetracene nanoparticles.

DLS results shows the presence of two populations of nanoparticles with the sizes mentioned in Table 6.

The TIPS Tetracene nanoparticles were found to be unstable in the presence of light and air, leading to a color change from pinkish orange to colorless. This is because of endoperoxide formation through an oxygen-mediated pathway(39) in presence of oxygen and in light, the molecule undergoes photodimerisation to generate a novel alkyne photoproduct as reported by Puro et.al(39).

<u>TA data analysis</u>

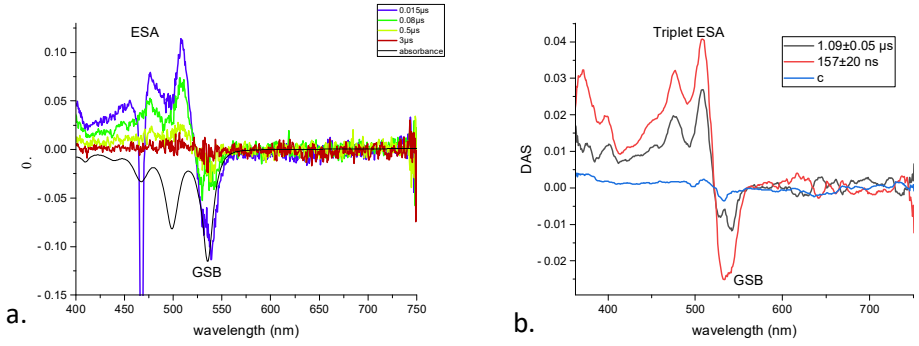

Fig 27.(a)Transient absorption results of deaerated TIPS Tetracene nanoparticle (b) Decay associated spectra obtained after fitting, excited at 467.5 nm, absorbance=0.6, power 20.4 mW, 1cm cuvette.

From the transient absorption spectra in fig 27(a), the Ground state bleach feature is observed at 536 nm which follows the Ground state absorption spectra and corresponds to $S_0 \rightarrow S_1$ 0-0 vibronic band. The spectra has intense ESA features at 470 and 510 nm, which corresponds to triplet excited states ($T_1 \rightarrow T_N$ transition), the shape of the spectra remains the same throughout. The decays at the 470 nm and 510 nm are the same. A global fit is used to fit the TA, and obtained lifetimes are $\tau1$=1.09±0.05 µs and $\tau2$= 157±20 ns for triplet states of two nanoparticle populations. A Triplet QY of 33% was obtained using the relative actinometry method using $[Ru(bpy)_3]^{2+}$ as a reference as explained previously.

Adding to that, freshly prepared nanoparticle solutions of TIPS Pentacene and TIPS Tetracene were non-emissive, which increases the probability of singlet fission in these molecules. Since, emission implies a relaxation pathway from the S_1 state to S_0 state, quenching of emission in nanoparticle solutions infers a higher efficiency of singlet fission possible as more singlet excited states will be available to undergo singlet fission. This quenched emission for nanoparticle solution when compared to solution in THF which is highly emissive is due to the singlet state being substantially quenched by a kinetically competitive intermolecular process as reported by Mauck et.al(40).

4.5. TIPS Anthracene in THF

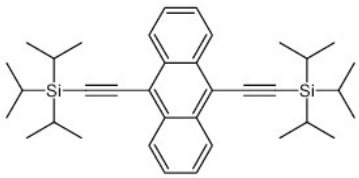

Fig 28. Structure of 9,10-Bis[(triisopropylsilyl)ethynyl]anthracene

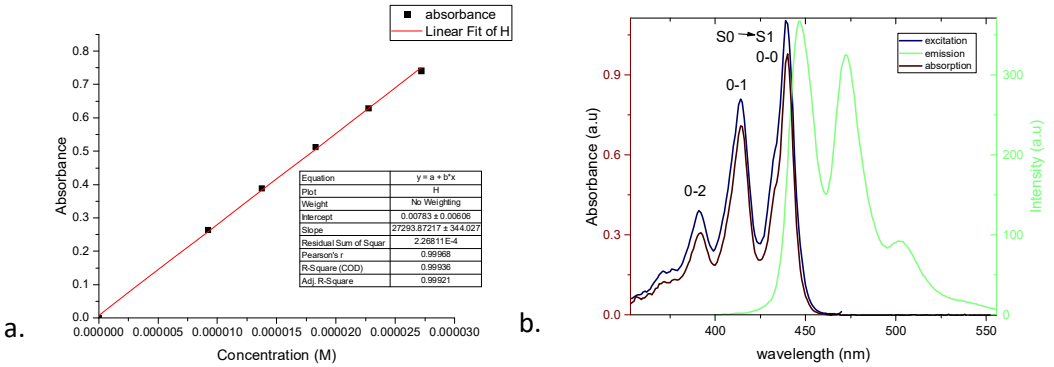

Fig 29. (a) Plot of absorbance vs concentration showing a linear dependence for an absorbance less than 1, thereby obtaining the molar extinction coefficient using Beer-Lambert's law (b). Absorption (brown), emission(green) and excitation(blue) spectrum of TIPS Anthracene in THF.

Fig 29(b). gives insights onto the absorption, excitation and emission characteristics of TIPS Anthracene in THF. The emission spectra is the mirror image of the absorption spectra and the excitation spectra overlaps with the absorption spectra. The characteristic peaks have been assigned from the literature as : $S_0 \rightarrow S_1$: 440 nm, 415 nm, 393 nm corresponding to 0-0, 0-1 and 0-2 vibronic transitions respectively. The emission features exhibit three peaks at 506 nm, 474 nm and 448 nm corresponding to the emission from $S_1 \rightarrow S_0$: 0-0, 0-1, and 0-2 vibronic

transitions respectively. The molar absorption coefficient at 415 nm is calculated to be 27300 M^{-1} cm^{-1}.

TA data analysis:

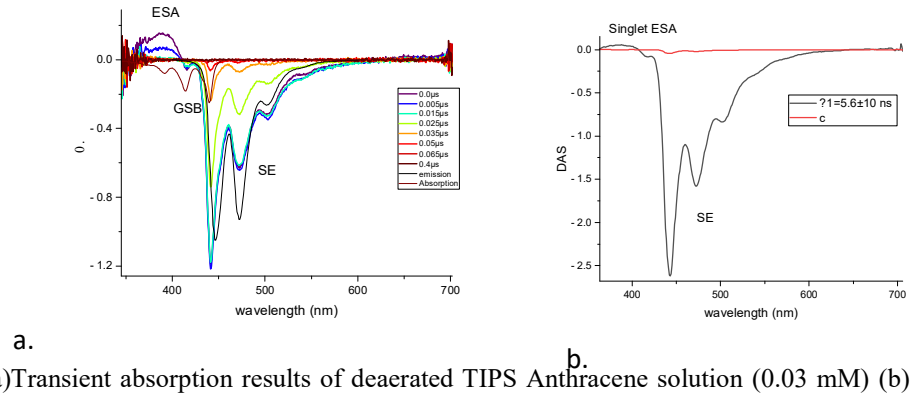

a. b.

Fig 30. (a)Transient absorption results of deaerated TIPS Anthracene solution (0.03 mM) (b) Decay associated spectra obtained after fitting, excited at 442 nm, absorbance = 0.35, power 1.4 mW, 4mm cuvette.

From the transient absorption spectra in fig30(a), the Ground state bleach feature is observed at 415 and 440 nm, which follows the Ground state absorption spectra and corresponds to S_0 → S_1 vibrational transitions of 0-1, and 0-0 transitions respectively. Similar to TIPS Tetracene, the solution of TIPS Anthracene is highly emissive in nature and hence low excitation pump powers were required to get spectra without having emission saturation. The stimulated emission features are observed at 506 nm, 474 nm and 448 nm, with the GSB and SE overlapping at the 506 nm. The spectra has ESA features at 390 nm, which corresponds to singlet excited states (S_1→ S_N transition) which decays rapidly. Triplet states are not detected in the solution. A global fit is used to fit the TA and obtained τ1=5.6±10 ns for the singlet state.

4.6. TIPS Anthracene nanoparticle

Nanoparticles of TIPS Anthracene were prepared through flash-precipitation as mentioned in the materials and methods section. Some studies have been made on Anthracene systems and it is found to undergo slightly endergonic singlet fission, similar to Tetracene, which occurs within the 100fs of excitation (24). Nanoparticle solution of the same was synthesized from a 1 mM stock solution in distilled THF in deaerated and dark conditions:

2 mL of stock solution was added to vigorously stirred 18 mL of distilled water leading to the formation of yellow colored nanoparticle solution.

In contrary to TIPS Pentacene and TIPS anthracene nanoparticle solutions, TIPS Anthracene nanoparticles were emissive (weakly) in nature.

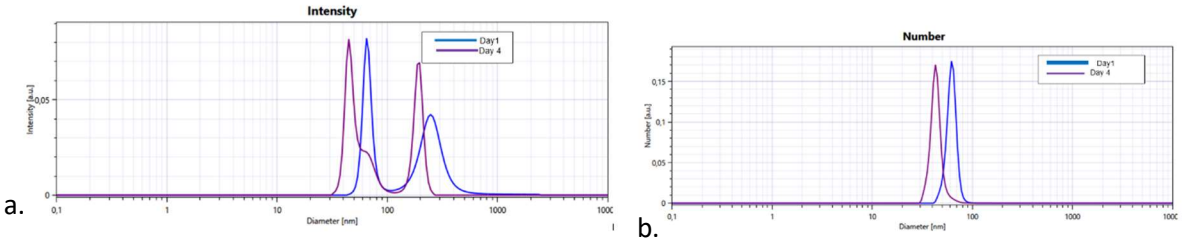

a. b.

Fig 31.DLS results of TIPS Anthracene nanoparticle over a span of 4 days, (a) SBL intensity, (b). SBL number.

TIPS Anthracene	SBL intensity (nm)	SBL number (nm)
Day 1	65, 247	62
Day 4	45, 196	43

Table 7. Size of nanoparticles obtained from DLS measurements over a span of 4 days for TIPS Anthracene nanoparticles.

DLS results shows the presence of two populations of nanoparticles with the sizes mentioned in Table 7.

TA data analysis

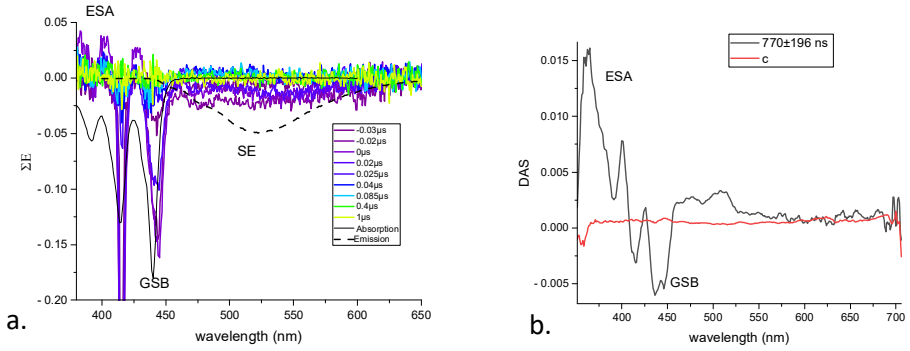

Fig 32. (a)Transient absorption results of degassed TIPS Anthracene nanoparticle solution (b) Decay associated spectra obtained after fitting, excited at 415 nm, absorbance=0.5, power 21 mW, 1 cm cuvette.

From the transient absorption spectra in fig 32(a), the Ground state bleach feature is observed at 440 nm, 415 nm, and 392 nm which follows the Ground state absorption spectra and corresponds to $S_0 \rightarrow S_1$ 0-0, 0-1, and 0-2 vibronic bands respectively. The spectra have very low ESA features at 382, 404, and 428 nm, which corresponds to triplet excited states ($T_1 \rightarrow T_N$ transition), which is confirmed by the literature (14). A global fit is used to fit the TA and a lifetime of $\tau 1$=770±196 ns is deduced for the triplet state. Eventhough having two populations of nanoparticles from DLS measurements, the absence of two lifetimes is attributed to the low intensity of triplet ESA obtained, which limited the data fitting.

SEM results: Morphological analysis of the TIPS Anthracene nanoparticle has been analyzed using SEM measurements, where the particles were square plate like stacked structure and had a size of 179±81 nm, upon statistical analysis using Image J software. The size distribution has been plotted in a histogram as shown in Fig 33. (b), the morphology of nanoparticles reveals that the nanoparticles are stacked together. The slightly increased size of the sample in SEM measurements, compared to those of the DLS, can be due to the difference in physical state of the particle. Similar to TIPS Pentacene, freeze-dried particles were used for SEM characterization and might have caused a slight increase in the particles.

a. 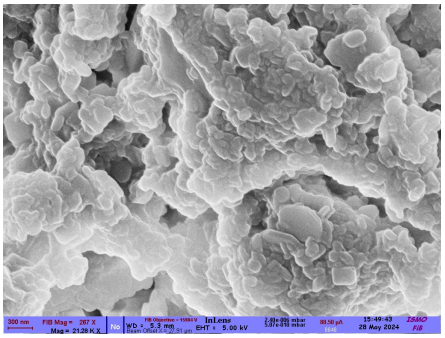

b. 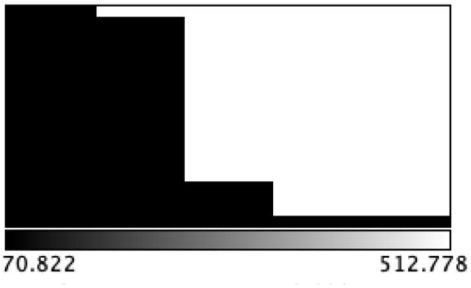

Fig 33.(a) SEM measurements of TIPS Anthracene nanoparticles, (b) Histogram of size distribution in µm scale.

Comparison between different nanoparticles

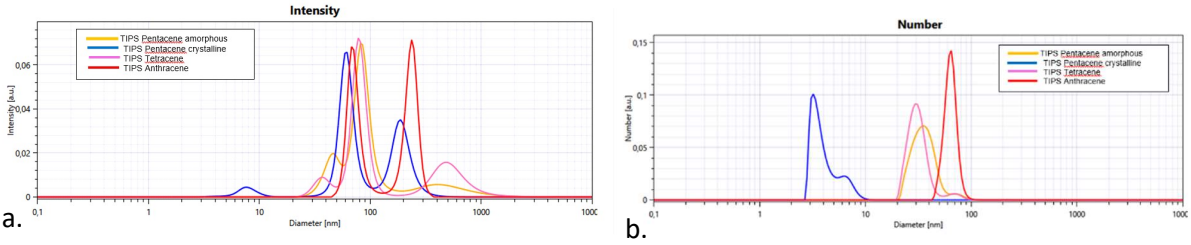

a. b.

Fig 34. DLS results of comparison of nanoparticles of crystalline TIPS Pentacene, amorphous TIPS Pentacene ,TIPS Tetracene and TIPS Anthracene (a) SBL intensity, (b) SBL number.

Nanoparticle	SBL intensity (nm)	SBL number (nm)	Lifetime	
TIPS Pentacene (amorphous)	46,82,412	35,71	965±20 ns	122±20 ns
TIPS Pentacene (crystalline)	8,62,187	3,6	857±76 ns	102±20 ns
TIPS Tetracene	37,78,495	29,71	1.09±0.05 µs	157±20 ns
TIPS Anthracene	68,236	65	770±196 ns	

Table 8. Comparison of size of nanoparticles obtained from DLS measurements for TIPS Pentacene(amorphous), TIPS Pentacene (crystalline), TIPS Tetracene and TIPS Anthracene.

The same synthesis method was employed for the nanoparticles of the acenes and, from the comparison of the DLS results, the sizes obtained for the freshly prepared samples are similar and range from 35-70 nm (Fig 34). The lifetimes obtained for the two nanoparticle populations are also similar for all three nanoparticles as tabulated in table 8.

Conclusion and Perspectives

Preliminary studies in solutions and nanoparticle solutions of the molecular systems exhibiting the singlet fission process have been carried out using nanosecond transient absorption spectroscopy. Photophysical investigations on a range of acenes were performed using UV-vis absorption, emission and nanosecond transient absorption spectroscopy. The nanoparticles of TIPS Pentacene, TIPS Tetracene, and TIPS Anthracene were synthesized successfully using the flash precipitation method. The sizes of the nanoparticles were measured using DLS and two populations of nanoparticles were obtained in each case with a size ranging from 40-80 nm. The addition of PVA resulted in the morphological evolution of amorphous to crystalline nanoparticles for TIPS Pentacene nanoparticle, which in turn led to strong intermolecular coupling between the chromophores and thereby Davydov splitting, whereas no effect was observed in TIPS Tetracene and TIPS Anthracene nanoparticles.

Nanosecond Transient absorption spectroscopy was employed to characterize the decay, signature, and lifetimes of singlet and triplet excited states. For the TIPS Pentacene solution in THF, a possible oxygen-catalyzed sequential singlet fission process was observed due to its low triplet energy than the singlet oxygen, whereas it is not the case for the other two acenes studied. Freshly prepared nanoparticle solutions of TIPS Pentacene and TIPS Tetracene had no emission, which suggests an increased probability of singlet fission in these molecules, since the emission effectively implies the relaxation of singlet excited state to the ground state, quenching of which will increase the probability of singlet fission process by outcompeting other relaxation pathways. Whereas, the TIPS anthracene nanoparticles were emissive in nature, thereby a good triplet intensity was not observed in the nanosecond scale, due to the relaxation through emission.

Morphological analysis using SEM measurements revealed the presence of brick-like particles for TIPS Pentacene nanoparticles and closely packed square plate-like nanoparticles for TIPS Anthracene, which reveals the presence of closely packed structure in these nanoparticles and effectively aids in stacked structures. SEM measurements gave the idea of morphology of the particles, which is non-spherical for the particles analyzed, while DLS assumes particles to have spherical shape for size analysis, and hence the sizes obtained through DLS and SEM differs.

Since, singlet fission is an ultrafast process that occurs in a sub-picosecond scale, the nanosecond transient absorption studies are only important to understand the signature and lifetime of the triplet states. Femtosecond transient absorption spectroscopy must be employed to further characterize the intermediate in the singlet fission process, and the associated mechanistic elucidations. My first femtosecond experiments were performed in the Harpia TA set up at the University of Lorraine, Nancy by the end of the internship. During the experiment, the expected signatures were presumably observed, and data analysis needs to be done in the near future.

Bibilography

1. Wollscheid N, Pérez Lustres JL, Kefer O, Hahn S, Brosius V, Bunz UHF, et al. Oxygen-catalysed sequential singlet fission. Nat Commun. 2019 Nov 15;10(1):5202.
2. Xia J, Sanders SN, Cheng W, Low JZ, Liu J, Campos LM, et al. Singlet Fission: Progress and Prospects in Solar Cells. Adv Mater. 2017 May;29(20):1601652.
3. Congreve DN, Lee J, Thompson NJ, Hontz E, Yost SR, Reusswig PD, et al. External Quantum Efficiency Above 100% in a Singlet-Exciton-Fission–Based Organic Photovoltaic Cell. Science. 2013 Apr 19;340(6130):334–7.
4. Baldacchino AJ, Collins MI, Nielsen MP, Schmidt TW, McCamey DR, Tayebjee MJY. Singlet fission photovoltaics: Progress and promising pathways. Chem Phys Rev. 2022 Jun 1;3(2):021304.
5. Textmap L. Physical Chemistry for the Biosciences.
6. Stern HL, Musser AJ, Gelinas S, Parkinson P, Herz LM, Bruzek MJ, et al. Identification of a triplet pair intermediate in singlet exciton fission in solution. Proc Natl Acad Sci. 2015 Jun 23;112(25):7656–61.
7. Basel BS, Zirzlmeier J, Hetzer C, Reddy SR, Phelan BT, Krzyaniak MD, et al. Evidence for Charge-Transfer Mediation in the Primary Events of Singlet Fission in a Weakly Coupled Pentacene Dimer. Chem. 2018 May;4(5):1092–111.
8. Farag MH, Krylov AI. Singlet Fission in Perylenediimide Dimers. J Phys Chem C. 2018 Nov 15;122(45):25753–63.
9. Liu Y, Yang X, Ye L, Ma H, Zhu H. Molecular stacking controlling coherent and incoherent singlet fission in polymorph rubrene single crystals: Special Issue: Emerging Investigators. Aggregate. 2023 Oct;4(5):e347.
10. Tayebjee MJY, Schwarz KN, MacQueen RW, Dvořák M, Lam AWC, Ghiggino KP, et al. Morphological Evolution and Singlet Fission in Aqueous Suspensions of TIPS-Pentacene Nanoparticles. J Phys Chem C. 2016 Jan 14;120(1):157–65.
11. Qiao X, Ma D. Nonlinear optoelectronic processes in organic optoelectronic devices: Triplet-triplet annihilation and singlet fission. Mater Sci Eng R Rep. 2020 Jan;139:100519.
12. Ni W, Sun L, Gurzadyan GG. Ultrafast spectroscopy reveals singlet fission, ionization and excimer formation in perylene film. Sci Rep. 2021 Mar 4;11(1):5220.
13. Stuart AN, Tapping PC, Kee TW, Huang DM. Pitfalls of quantifying intersystem crossing rates in singlet-fission chromophore solutions. J Chem Phys. 2022 Aug 28;157(8):084312.
14. de Clercq DM, Collins MI, Sloane NP, Feng J, McCamey DR, Tayebjee MJY, et al. Singlet fission in TIPS-anthracene thin films. Chem Sci. 2024;10.1039.D3SC06774B.
15. Eaton SW, Shoer LE, Karlen SD, Dyar SM, Margulies EA, Veldkamp BS, et al. Singlet Exciton Fission in Polycrystalline Thin Films of a Slip-Stacked Perylenediimide. J Am Chem Soc. 2013 Oct 2;135(39):14701–12.
16. Lim SH, Bjorklund TG, Spano FC, Bardeen CJ. Exciton Delocalization and Superradiance in Tetracene Thin Films and Nanoaggregates. Phys Rev Lett. 2004 Mar 12;92(10):107402.
17. Tayebjee MJY, Clady RGCR, Schmidt TW. The exciton dynamics in tetracene thin films. Phys Chem Chem Phys. 2013;15(35):14797.
18. Wang L, Cai W, Sun J, Wu Y, Zhang B, Tian X, et al. H-Type-like Aggregation-Accelerated Singlet Fission Process in Dipyrrolonaphthyridinedione Thin Film: The Role of Charge Transfer/Excimer Mixed Intermediate State. J Phys Chem Lett. 2021 Dec 30;12(51):12276–82.
19. Walker BJ, Musser AJ, Beljonne D, Friend RH. Singlet exciton fission in solution. Nat Chem. 2013 Dec;5(12):1019–24.
20. Dvořák M, Prasad SKK, Dover CB, Forest CR, Kaleem A, MacQueen RW, et al. Singlet Fission in Concentrated TIPS-Pentacene Solutions: The Role of Excimers and Aggregates. J Am Chem Soc. 2021 Sep 1;143(34):13749–58.
21. Barlier VS, Schlenker CW, Chin SW, Thompson ME. Acetylide-bridged tetracene dimers. Chem Commun. 2011;47(13):3754.
22. Avalos CE, Richert S, Socie E, Karthikeyan G, Casano G, Stevanato G, et al. Enhanced Intersystem Crossing and Transient Electron Spin Polarization in a Photoexcited Pentacene–Trityl Radical. J Phys Chem A. 2020 Jul 23;124(29):6068–75.
23. He Z, Chen J, Keum JK, Szulczewski G, Li D. Improving performance of TIPS pentacene-based organic thin film transistors with small-molecule additives. Org Electron. 2014 Jan;15(1):150–5.
24. Hudson RJ, de la Perrelle JM, Pensack RD, Kudisch B, Scholes GD, Huang DM, et al. Organizing Crystalline Functionalized Pentacene Using Periodicity of Poly(Vinyl Alcohol). J Phys Chem Lett. 2020 Jan 16;11(2):516–23.
25. Stuart AN, Tapping PC, Schrefl E, Huang DM, Kee TW. Controlling the Efficiency of Singlet Fission in TIPS-Pentacene/Polymer Composite Nanoparticles. J Phys Chem C. 2019 Mar 14;123(10):5813–25.
26. Pensack RD, Grieco C, Purdum GE, Mazza SM, Tilley AJ, Ostroumov EE, et al. Solution-processable, crystalline material for quantitative singlet fission. Mater Horiz. 2017;4(5):915–23.
27. Basel BS, Hetzer C, Zirzlmeier J, Thiel D, Guldi R, Hampel F, et al. Davydov splitting and singlet fission in excitonically coupled pentacene dimers. Chem Sci. 2019;10(13):3854–63.
28. Busby E, Berkelbach TC, Kumar B, Chernikov A, Zhong Y, Hlaing H, et al. Multiphonon Relaxation Slows Singlet Fission in Crystalline Hexacene. J Am Chem Soc. 2014 Jul 30;136(30):10654–60.
29. Rao A, Wilson MWB, Hodgkiss JM, Albert-Seifried S, Bässler H, Friend RH. Exciton Fission and Charge Generation via Triplet Excitons in Pentacene/C $_{60}$ Bilayers. J Am Chem Soc. 2010 Sep 15;132(36):12698–703.
30. Pensack RD, Tilley AJ, Parkin SR, Lee TS, Payne MM, Gao D, et al. Exciton Delocalization Drives Rapid Singlet Fission in Nanoparticles of Acene Derivatives. J Am Chem Soc. 2015 Jun 3;137(21):6790–803.
31. Qian Y, da Silva A, Yu E, Anderson CL, Liu Y, Theis W, et al. Crystallization of nanoparticles induced by precipitation of trace polymeric additives. Nat Commun. 2021 May 13;12(1):2767.
32. What can't it do? - SEM [Internet]. [cited 2024 Jul 11]. Available from: https://myscope.training/SEM_What_can_t_it_do
33. Arenas-Guerrero P, Delgado ÁV, Donovan KJ, Scott K, Bellini T, Mantegazza F, et al. Determination of the size distribution of non-spherical nanoparticles by electric birefringence-based methods. Sci Rep. 2018 Jun 22;8(1):9502.
34. Karlsson JKG, Atahan A, Harriman A, Tojo S, Fujitsuka M, Majima T. Pulse Radiolysis of TIPS-Pentacene and a Fluorene-bridged Bis(pentacene): Evidence for Intramolecular Singlet-Exciton Fission. J Phys Chem Lett. 2018 Jul 19;9(14):3934–8.
35. Angew Chem Int Ed - 2017 - Mendes Marinho - Time-Resolved Interception of Multiple-Charge Accumulation in a Sensitizer.pdf.
36. Ishibashi Y, Inoue Y, Asahi T. The excitation intensity dependence of singlet fission dynamics of a rubrene microcrystal studied by femtosecond transient microspectroscopy. Photochem Photobiol Sci. 2016 Oct;15(10):1304–9.
37. Allardice JR, Thampi A, Dowland S, Xiao J, Gray V, Zhang Z, et al. Engineering Molecular Ligand Shells on Quantum Dots for Quantitative Harvesting of Triplet Excitons Generated by Singlet Fission. J Am Chem Soc. 2019 Aug 14;141(32):12907–15.
38. Thampi A, Stern H, Cheminal A, Anthony J, Rao A. Ultrafast dynamics of singlet fission in tips- tetracene nanoparticles.
39. Puro R, Van Schenck JDB, Center R, Holland EK, Anthony JE, Ostroverkhova O. Exciton Polariton-Enhanced Photodimerization of Functionalized Tetracene. J Phys Chem C. 2021 Dec 16;125(49):27072–83.
40. Mauck CM, Hartnett PE, Wu YL, Miller CE, Marks TJ, Wasielewski MR. Singlet Fission within Diketopyrrolopyrrole Nanoparticles in Water. Chem Mater. 2017 Aug 22;29(16):6810–7.